

TOPOLOGY OPTIMIZATION OF COMPLIANT MECHANISMS FOR SEISMIC ISOLATION OF SPATIAL STRUCTURES

Takuya Kinoshita¹⁾, Makoto Ohsaki²⁾ and Taku Nakajima¹⁾

1) Graduate Student, Kyoto University, Kyoto, Japan

2) Associate Professor, Kyoto University, Kyoto, Japan

ABSTRACT

An optimization approach is developed for design of base-isolation device for vertical motions. A method is first presented for optimizing a compliant bar-joint structure that has the nonlinear equilibrium path close to the specified shape. Numerical examples of a long-span arch-type truss demonstrates the validity of the compliant bar-joint structure as the isolation system for vertical seismic motions.

1. INTRODUCTION

The structures in civil and architectural engineering are usually designed so as to resist external loads with enough stiffness. On the other hand, a *mechanism* produces output displacements as desired using an unstable motion. By contrast, a *compliant mechanism* is designed so that it achieves the required deformation utilizing the flexibility (elastic deformation) of the members and joints of the structure.

For example, Ohsaki and Nishiwaki [1] presented an optimization method for generating a compliant bar-joint structure that produces large output deformation utilizing snapthrough behavior. A compliant mechanism can also be used for realizing the structure that has a specified nonlinear equilibrium path (load-displacement relation) [2]. In this study, we utilize compliant mechanism for the design of base-isolation of spatial structures in the vertical direction.

In most of the base-isolation systems in civil and architectural engineering, the horizontal motions are isolated using the flexible supports and/or sliding devices. It is very difficult, however, to isolate the vertical motion, because, in this case, the flexibility against seismic motions and stiffness against the gravity load are simultaneously required. Several systems have been developed for this purpose [3, 4]; however, they require special materials, and it is very difficult to apply them to large-scale structures. For isolation of high-precision machines, a simple compli-

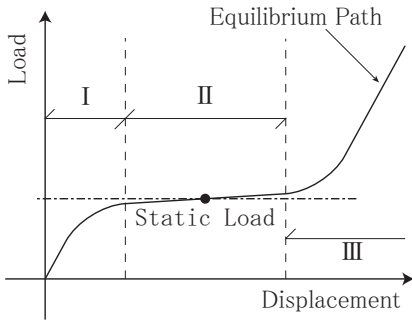


Fig.1. Equilibrium path with gradually increasing load region.

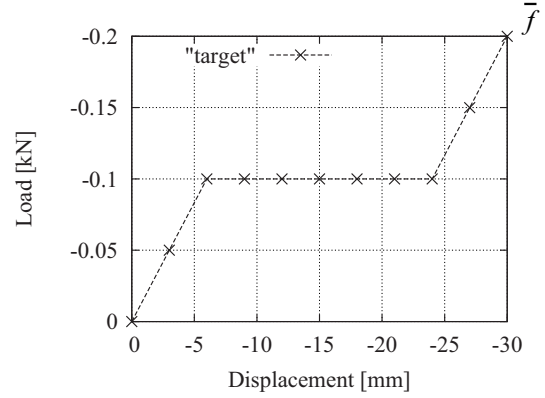


Fig.2. Discretized target equilibrium path.

ant bar-joint system has been developed for three-dimensional isolation table [5].

In this study, we first present an approach to optimizing compliant bar-joint system to have the specified nonlinear equilibrium path. The method is applied to design of flexible support for a spatial structure for isolating vertical seismic motions with enough stiffness against the gravity load. The effectiveness of the proposed mechanism is investigated for a long-span arch subjected to white noise and recorded ground motions.

2. OPTIMAL DESIGN SPECIFYING EQUILIBRIUM PATH

2.1 Problem Formulation

In this section, we propose a method for designing a compliant bar-joint structure that has the specified nonlinear load-displacement relation. In order to use the mechanism for base-isolation, the relation between the input force $f(U_A)$ and the displacement U_A at the input node 'A' is given as shown in Fig. 1. The structure has moderately large stiffness in regions I and III to prevent too large drift without a retaining wall against unexpectedly large seismic motions. The equilibrium point under gravity load (self-weight of the upper structure) is expected to be at the center of the region II with very small tangential stiffness. The stiffness in region I should be moderately large also for preding large deformation against the self-weight.

The ground structure approach is used for generating the mechanism through optimization of cross-sectional areas. Note that the nodal locations are also optimized as the variables. We first divide the target equilibrium path by m points; e.g., 10 points excluding the origin as shown in Fig. 2. The displacement and the specified force at the i th point are denoted by $U_A^{(i)}$ and \bar{f}_i , respectively. The error e , defined as follows, of the load $f(U_A^{(i)})$, computed by a path-tracing analysis, from the specified value \bar{f}_i is minimized:

$$e = \sum_{i=1}^m (f(U_A^{(i)}) - \bar{f}_i)^2 \quad (1)$$

The region II defined by the interval $\bar{U}_A^{(l)} \leq U_A \leq \bar{U}_A^{(u)}$ has gradually increasing load as

$$f(U_A^{(i)}) \leq f(U_A^{(i+1)}), \quad (i = l, \dots, u - 1) \quad (2)$$

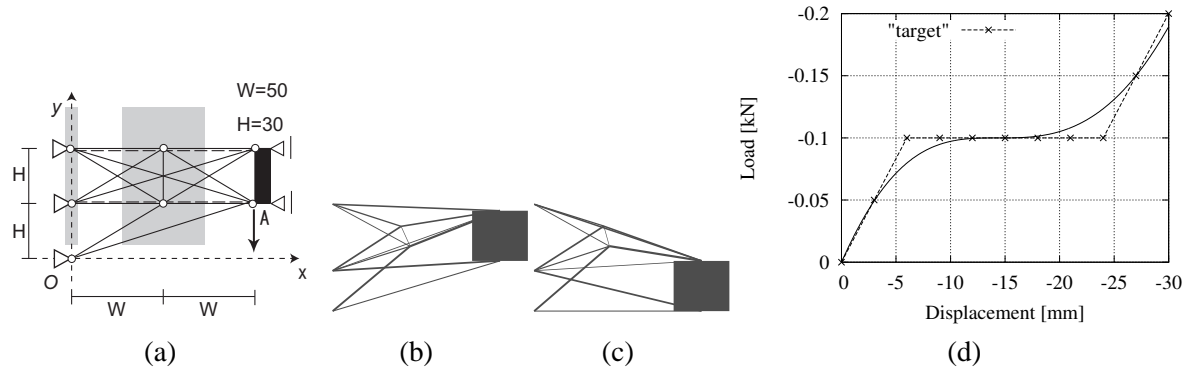


Fig.3. Optimal solution with Model-1. (a) Model-1, (b) Undeformed configuration, (c) Deformed configuration, (d) Equilibrium path.

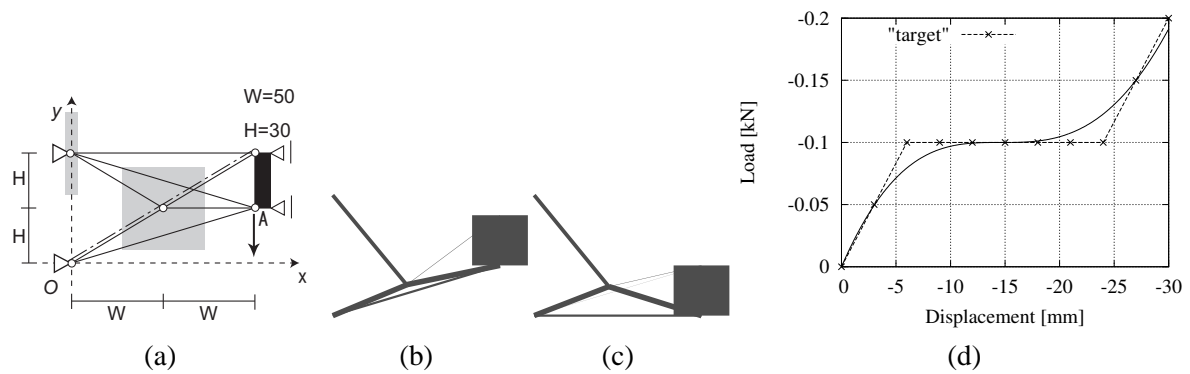


Fig.4. Optimal solution with Model-2. (a) Model-2, (b) Undeformed configuration, (c) Deformed configuration, (d) Equilibrium path.

Let \mathbf{X} and \mathbf{A} denote the nodal coordinates and the cross-sectional areas of the members. Then $U_A^{(i)}$ and e are the functions of \mathbf{X} and \mathbf{A} . Let V^{\max} denote the upper bound of the total structural volume $V(\mathbf{X}, \mathbf{A})$, i.e.,

$$V(\mathbf{X}, \mathbf{A}) \leq V^{\max} \quad (3)$$

The upper and lower bound of the variables are indicated by $(\cdot)^U$ and $(\cdot)^L$, respectively. Then the optimization problem is formulated as

$$\text{Minimize } e(\mathbf{X}, \mathbf{A}) \quad (4)$$

$$\text{subject to } (2), (3)$$

$$\mathbf{A}^L \leq \mathbf{A} \leq \mathbf{A}^U \quad (5)$$

$$\mathbf{X}^L \leq \mathbf{X} \leq \mathbf{X}^U \quad (6)$$

2.2 Truss Model

Optimal solutions are found from the ground structures as shown in Fig. 3(a) (Model-1) and Fig. 4(a) (Model-2), respectively, where the gray regions are feasible regions of the nodes, and the filled region is a rigid body. A forced displacement $U_A=30$ (mm) is applied at node 'A'. Each member is modeled by truss element, and the rigid body is modeled also using truss elements

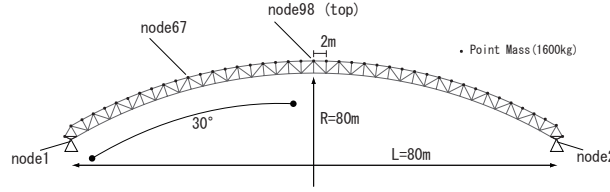


Fig.5. An arch model.

with sufficiently large cross-sectional areas. Note that appropriate springs should be used for flexible members, especially for members in compression; however, we use truss element, and buckling or yielding is not considered.

The co-rotational formulation with engineering strain is used for geometrically nonlinear analysis. The elastic modulus is 2.0 kN/mm^2 . The displacement increment method with increment 0.05 mm is used for path-tracing analysis, and the unbalanced load is canceled at the subsequent step without iterative correction.

The initial value Fig. 3(a) and Fig. 4(a) show the initial location X^0 of the nodes. The upper and lower bound for the variable nodal coordinate X_i are given as $X_i^0 \pm 20 \text{ (mm)}$. The the initial value and the upper and lower bound (mm^2) for the cross-sectional area are 1.0, 100, and 0.01, respectively, and V^{\max} is $5000 \text{ (mm}^3\text{)}$.

2.3 Design Algorithm

Optimal compliant bar-joint structures are found using the optimization package IDESIGN [7] that utilizes sequential quadratic programming. The sensitivity coefficients are computed using a finite difference approach. Since this optimization problem is highly nonlinear, the best solution is selected from the optimal solutions from 100 different initial solutions. The initial value of the cross-sectional area is given as $A_i = 1.0 + (R_i - 0.5)$ with a uniform random number $R_i \in [0, 1)$. Also for the variable nodal coordinate x_i , the initial value is given as $x_i = x_i^0 + 20.0(R_i - 0.5)$ with the location x_i^0 in Fig. 3(a) and Fig. 4(a). The initial values of the y-coordinates are given similarly. Note that the optimization process is terminated if convergence is not achieved within 50 iterations.

2.4 Optimal Solutions

Optimization results are shown in Fig. 3(b)–(d) and Fig. 4(b)–(d), where the width of each member in Fig. 3(b),(c) and Fig. 4(b),(c) is proportional to its cross-sectional area, and the member with $A_i = A_i^L$ are removed. The objective values of the best solutions of Model-1 and Model-2 are 6.80×10^{-2} and 6.65×10^{-2} , respectively, which indicates good approximation of the specified equilibrium path. Note that a simpler solution is obtained from Model-2 that has fewer members than Model-1. The number of converged solutions out of 100 trials is 64 for Model-1 and 87 for Model-2.

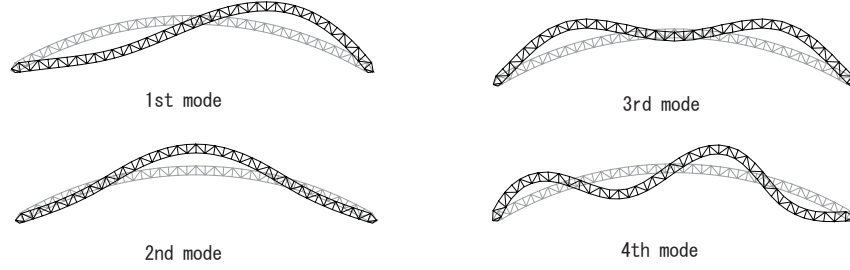


Fig.6. Four lowest eigenmodes; natural periods (s) $T_1 = 1.21$, $T_2 = 2.27$, $T_3 = 3.88$, $T_4 = 4.52$)

Table 1. Maximum response against white noises

white noise	Arch	Arch + Spring			Arch + Device		
	Acc_{98}^{\max}	Δ^{\max}	Acc_{98}^{\max}	ratio	Δ^{\max}	Acc_{98}^{\max}	ratio
w01	4.837	0.370	0.923	0.191	0.224	0.551	0.114
w02	5.380	0.158	0.415	0.077	0.234	0.842	0.156
w03	5.314	0.150	0.384	0.072	0.178	0.423	0.080
w04	5.661	0.291	0.724	0.128	0.124	0.124	0.022
w05	3.905	0.133	0.342	0.088	0.232	0.557	0.143

3. SEISMIC ISOLATION SYSTEM

A supporting structure is designed to vertically isolate a long-span roof from the lower boundary structure. The roof is modeled by a 2-dimensional circular arch as shown in Fig. 5. See Ref. [6] for detail of the model. Fig. 6 shows the lowest four modes.

A base-isolation device is designed from Model-3 shown in Fig. 7(a), where the optimization algorithm and the parameter values are same as those in Sec. 2. The optimization results are shown in Fig. 7(b),(c).

The optimal solution is scaled so that its width is 1 m and the elastic modulus is 2×10^{10} Pa. The cross-sectional areas of all members are multiplied by 321.0 so that the equilibrium point under gravity load exists at the center of the region II. If the supporting structure is modeled by a single-degree-of-freedom structure and the upper arch is assumed to be rigid, then the stiffness is 27.93×10^3 N/m, and the natural period is 6.97 s. This model is attached at the two supports of the arch.

The responses against vertical motions of the base-isolated structure are compared with those of the pin-supported structure. The finite element analysis software package ABAQUS Ver. 6.5 is used for analysis. Since the symmetric second and third modes are excited by a vertical motion, the parameters for the Rayleigh damping is defined so that the damping factors are 0.02 for $T_2 = 2.27$ and $T_3 = 3.88$ of the pin-supported structure.

Let Acc_g^{\max} denote the maximum ground acceleration. In the following ‘maximum value’ means ‘maximum absolute value’, for brevity. The maximum acceleration of node i is denoted by Acc_i^{\max} . The response ratio is defined as the ratio of Acc_{98}^{\max} of the center node indicated in Fig. 5 of the base-isolated structure to that of the pin-supported structure. The maximum displacement of the base-isolation device is denoted by Δ^{\max} .

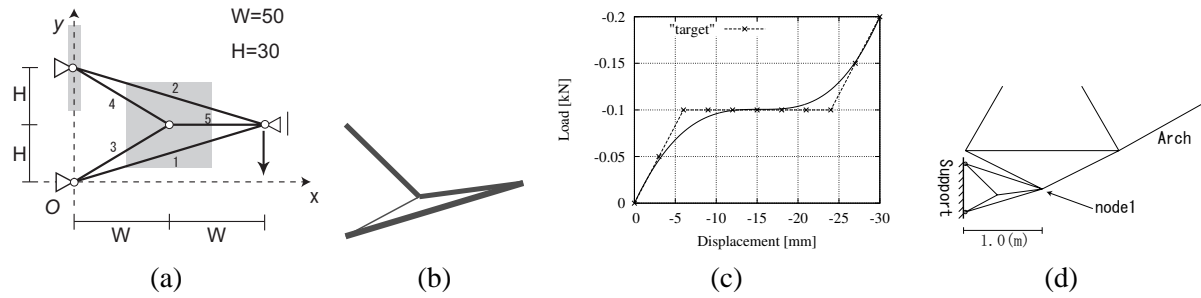


Fig.7. Optimal solution with Model-3. (a) Model-3, (b) Undeformed configuration, (c) Equilibrium path, (d) Connection with spatial structure.

Table 2. Maximum response against record waves.

Wave	Arch				Arch + Spring				Arch + Device			
	Acc_g^{\max}	Acc_{67}^{\max}	Acc_{98}^{\max}	Δ^{\max}	Acc_{67}^{\max}	Acc_{98}^{\max}	ratio	Δ^{\max}	Acc_{67}^{\max}	Acc_{98}^{\max}	ratio	
(i) ₂	3.084	6.004	5.109	0.236	0.580	0.594	0.116	0.290	0.613	0.627	0.123	
(ii) ₂	1.627	12.557	6.223	0.135	0.336	0.347	0.056	0.394	1.732	1.803	0.290	
(iii) ₂	2.906	12.186	9.524	0.402	0.989	1.010	0.106	0.327	1.039	1.132	0.119	
(i) ₃	4.626	8.989	7.651	0.285	0.708	0.706	0.092	0.489	2.977	3.139	0.410	
(ii) ₃	2.440	18.860	9.405	0.203	0.505	0.521	0.055	0.408	1.674	1.748	0.186	
(iii) ₃	4.359	18.222	14.213	0.473	1.217	1.234	0.087	0.387	1.417	1.464	0.103	
(iv)	2.793	9.403	7.123	0.102	0.263	0.269	0.038	0.133	0.108	0.110	0.015	

4. ISOLATED RESPONSE AGAINST WHITE NOISE

We first investigate the responses against the white noise. Five types w01–w05 of white noise are generated using random numbers of normal distribution $N(0, 1)$ from five different random seeds. The white noises are scaled so that the maximum accelerations are equal to 3.0 m/s^2 .

To determine the width of the region II with gradually increasing load, response analysis is carried out for the arch with linear spring with the period 4 second when attached to the supports. The responses are listed in Table 1. As is seen, the displacement and acceleration are successfully reduced. Since the maximum elongation of the spring is 0.370 m, the base-isolation device is designed so that it has the region II ranging $\pm 0.370 \text{ m}$ from the static equilibrium point. Note that the width of the region II of the compliant bar-joint structure designed from Model-3 is 0.18 m. Therefore, the member lengths are scaled by $(2 \times 0.37)/0.18 = 4.11$. Hence, the width and height of the device are 4.11 m and 2.47 m, respectively, the elastic modulus is $2 \times 10^{10} \text{ Pa}$, and the maximum cross-sectional area is $3.39 \times 10^{-3} \text{ m}^2$.

Using this device, the responses against white noise are obtained as shown in Table 1. As is seen, the acceleration is drastically reduced by attaching the device. It is confirmed that the maximum displacement of the device is less than 0.370 m. However, the size $4.11 \text{ m} \times 2.47 \text{ m}$ is rather too large as a support structure.

5. ISOLATED RESPONSE AGAINST RECORDED MOTION

We next investigate the responses against the recorded seismic motions; (i) El centro UD (1940), (ii) Hachinohe UD (1968), and (iii) Taft UD (1952), each of which is scaled to the maximum velocity 0.50 m/s and 0.75 m/s, respectively, corresponding to level-1 and level-2 inputs; i.e.,

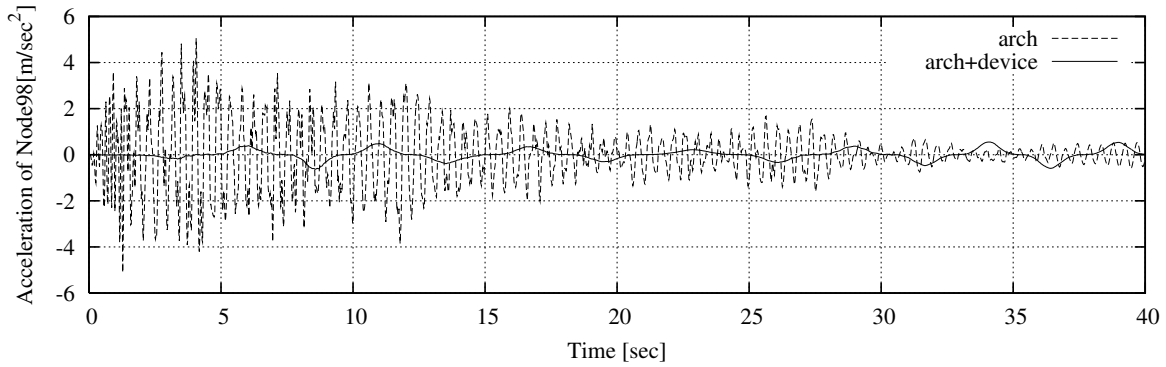


Fig.8. Acceleration response at node-98 against El centro UD (solid: isolated, dashed: pin-supported).

we have six motions in total. Furthermore, (iv) Takatori UD (1995) is used as a level-3 input without scaling. The maximum responses to these motions are listed in Table 2.

The maximum displacement for level-2 motions of the structure with linear spring is 0.402 m. Therefore, the size of the device is scaled by $(2 \times 0.402)/0.18 = 4.46$; hence, the width and height are 4.46 m and 2.68 m, respectively, the elastic modulus is 2×10^{10} Pa, and the maximum cross-sectional area is 3.39×10^{-3} m².

The time history of the acceleration response of node 98 to El centro UD (level-2) is plotted in Fig. 8. As is seen, the maximum acceleration is drastically reduced by attaching the device, and low-frequency vibration dominates in the response. The results for all motions are listed in Table 2. Note that the response ratio for level-2 motions are less than 0.3, and the maximum displacement of the device is less than 0.402 m. For level-3, the response ratios are less than 1.0 for all cases. However, also for this case, the size of the device is rather too large for a practical application.

6. CONCLUSION

An optimization method has been presented for optimization of a flexible truss called compliant bar-joint structure to have the nonlinear equilibrium path close to the specified shape. Using this method, a structure that has a region of gradually increasing load with sufficiently large initial and final stiffness can be obtained.

The proposed method has been applied for generating the vertical base-isolation device for spatial structures. It has been confirmed in the numerical examples of an arch-type truss that the responses to the vertical motions are successfully reduced by using the device designed by the proposed method.

REFERENCES

1. M. Ohsaki and S. Nishiwaki, Shape design of pin-jointed multistable compliant mechanisms using snapthrough behavior, *Struct. Multidisc. Optim.*, Vol. 30, pp. 327–334, 2005.
2. T. Seckimoto and H. Noguchi, Homologous topology optimization in large displacement

and buckling problems, *JSME International Journal, Series A*, Vol. 44, No. 4, pp. 616–622, 2001

3. T. Kamiya, K. Shingu, T. Irie, Y. Aoki, T. Kawashima and K. Mitsui, A study on vibration control of a structure with springs made of shape memory alloy, *Prof. Annual Conf., AIJ, Struct. Eng. I*, pp. 907–908, 2002. (in japanese)
4. T. Asai, N. Yoshida, T. Masui and Y. Araki, Vertical seismic isolation device using constant load supporting mechanism, *J. Struct. Constr. Eng., AIJ*, Vol. 73(631), pp. 1511–1518, 2008. (in japanese)
5. M. Ueda, K. Ohmata, R. Yamagishi and J. Yokoo, Vertical and three-dimensional seismic isolation tables with bilinear spring force characteristics, *J. JSME, Part C*, Vol. 73(735), pp. 60–67, 2007. (in japanese)
6. A. Uchida, M. Ohsaki and J. Y. Zhang, Prediction of inelastic seismic responses of spatial structures by static analysis with higher modes, *J. Struct. Eng.*, Vol. 55B, 2009, in press. (in japanese)
7. J. S. Arora and C. H. Tseng, *IDESIGN User's Manual*, Optimal Design Laboratory, University of Iowa, 1987.